Causal effect of covid vaccination on mortality in Europe

Article · February 2023

CITATIONS
2

READS
6,632

1 author:

André Redert
Rodotti
46 PUBLICATIONS **827** CITATIONS

SEE PROFILE

Causal effect of covid vaccination on mortality in Europe

André Redert, PhD
Independent researcher
Rodotti, Netherlands, 24 February 2023

Abstract

This report investigates short-term causal vaccine-mortality interactions during booster campaigns in 2022 in 30 European countries (population ~530M). An infection-vaccination-mortality model is introduced with causal aspects of repeatability, random chance, temporal order and confounding. The model is simple, has few or even zero prior model parameters and is unbiased in causal mechanisms and strengths. Confounders are taken into account explicitly of mortality-caused fear incentivizing vaccinations and four related to covid infections, and generically for all long-term confounding. Bayesian probabilities quantify all interactions, and from observed weekly administered vaccine doses and all-cause mortality, mortality on short-term *caused* by a vaccination dose is estimated as Vaccine Fatality Ratio (VFR).

VFR results are 0.13% (0.05%-0.21%, 95% confidence interval) in The Netherlands and 0.35% (0.15%-0.55%) in Europe, subtantially transcending covid IFR. Additionally, sewer-viral-particle experiments suggested vaccination induces covid-infections and/or reactivates latent viral reservoirs.

The evidence of a causal relationship from vaccination to both infection and mortality is a very strong alarm signal to immediately *stop* current mass vaccination programmes.

Statement of Interest

I declare that this work was done with an interest in science, and personal safety for myself, loved ones, and humanity. Pro bono, independent, without payroll, not funded. The only competing interest was time taken from my normal job (indy app developer in entertainment and music). If you want to support my work, feel free to buymeacoffee.com/AndreRedert, or consider one of the apps at rodotti.nl and qneo.net.

1. Introduction

Since the covid vaccination campaigns, high unexplained excess mortality rates have been observed worldwide, starting in the second half of 2021. In The Netherlands (population ~18M), excess mortality rates went up to ~80 people/day (excess ~20%) at end of 2022, before rising even more due to influenza. Based on the sparse publicly available Dutch data on mortality and vaccination, excess mortality was found to correlate positively with vaccination on long-term [Re1], and short-term [Mee,Sch,Re2]. Figure 1 illustrates this correlation for weekly 4th/5th vaccination campaign doses and all-cause mortality. Detailed case-based data has still not been made publicly available, and it remains a scientific challenge to analyse excess mortality using the sparse data that is both available, and reliable.

This report has the same goal as my earlier work [Re2], estimating short-term Vaccine Fatality Ratio (VFR) on the basis of weekly administered vaccine doses and all-cause mortality; two integer, countable parameters that do not suffer from the subjectivity and ambiguities in PCR testpolicies, covid diagnoses, cause of death atttributions, and modeling in mortality prognoses.

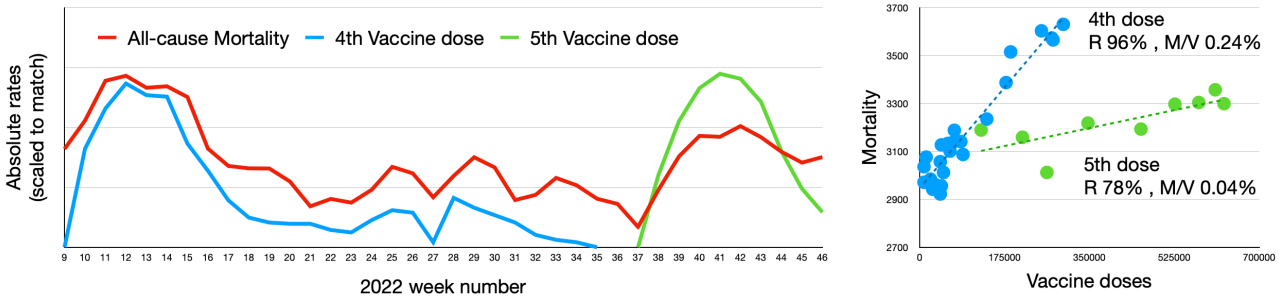

Figure 1: Left) Weekly rates in the Netherlands for mortality and administered covid vaccine doses [Src], scaled to illustrate temporal correlations. Right) Pearson correlations are very high. Different regression factors may be related to the campaigns' target ages (60+ and 12+).

New in this report is explicit causal modeling on the basis of repeatability, temporal order, handling of infection-based and generic confounders in a combined infection-vaccine-mortality (IVM) model, and the Bayesian framework to handle randomness and all statistic parameter estimation. The extraction of short-term events introduced in [Re2] to remove effects and confounding on long-term, see Figure 2, will be reused.

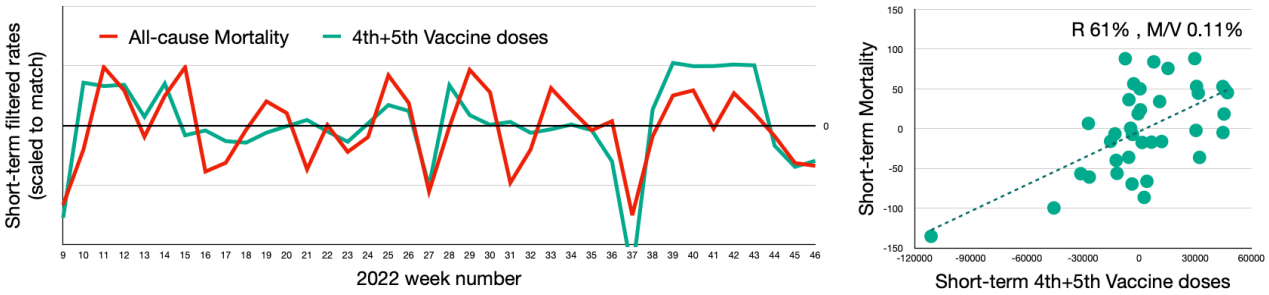

Figure 2: Same data as in Figure 1, short-term filtered to extract random weekly variations, easing a single analysis with multiple campaigns combined.

Infection data will be used of PCR tests and viral particle presence in sewer wastewater [Med], see Figure 3. As PCR tests are unreliable (false positives/negatives, test-willingness/policy-dependence, arbitrary CT-values, etc), and sewer data is more objective but less widely available, the relative performance of a simplified vaccine-mortality (VM) model without infections will be evaluated to widen the applicability of the method. Experiments will be performed for booster campaigns in 2022, in The Netherlands as well as 30 European countries (population ~530M).

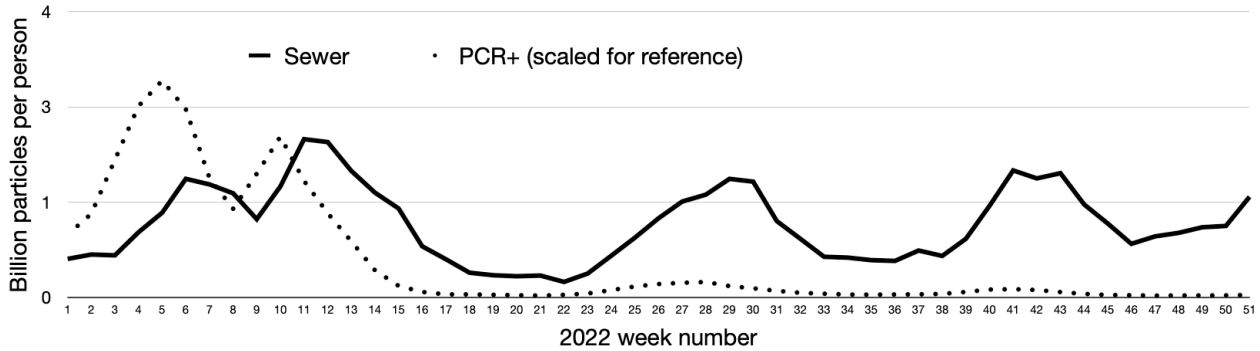

Figure 3: PCR+ tests and viral particle presence in sewer wastewater, The Netherlands. Sewer data may be more objective, but lags PCR+ infections by a few weeks, and also lags vaccinations and mortality as in Figure 1.

2. Method

In the next sections I will present my method in many high-detailed steps. The final result, however, is simple and contains a bare minimum, or even zero, model parameters.

2.1 Causality

The well-known "Correlation does not mean causation" is a *vague statement* that may lead to the false believe that all correlation is insufficient as evidence of causation. However, correlation is all one can observe, there *is* no alternative to determine causality. Pure causality cannot directly be observed as it is an "abstract philosophical concept that indicates how the world progresses" [Wik]. One can easily defend that:

"The origin of all correlation is causality"

The well-known vague statement means that when A and B are correlating, causation may not be between A and B (in either direction) but may involve a common cause known as a confounder. Correlations may also occur by chance, when an "oracle" set of events in the universe conspires to create the correlation; a confounder that cannot be known by definition, referred to by "random". Theoretically, such a random oracle could exist for every possible A and B, thereby pulling any practical use of causality out of the scientific realm[1].

Requirements for establishing causality have been studied for epidemiology in particular, listing consistency and strength of association, confounding, temporality, experiments and plausibility, based on the famous Bradford Hill criteria [Io1, Shi]. *Consistency and strength of association* can be rephrased as strong correlation, which can readily be observed in Figures 1 and 2. *Repeatability*, or rechallengable, and random chance are already essential ingredients in correlation analyses; e.g. covariances are characterizations of commonalities in many repeated observations, and statistical techniques exist to obtain mean and deviation of such covariances. *Temporality*, also known as temporal or causal ordering, and *confounding* are unique for causality, the reason to include these in my prior work [Re2] via a causality test involving temporal correlation and short-term-filtered observations to remove all long-term confounding.

In controlled *experiments,* one can make event A occur at will, which is very effective for excluding chance and confounders. Observational studies like in this report can, however, still accomplish the same goal via additional requirements (see also e.g. [Gia]): natural repeated occurrence of A, appropriately patterned in time to enable detection of the same pattern later in B according to temporal order, plus more emphasis on excluding a confounder/chance origin of the observed pattern. Finally, *plausability* requires a known mechanism that makes A cause B. For current covid vaccines, there are plenty of plausible mechanisms that lead to mortality, e.g. acute myo/pericarditis later followed by sudden cardiac arrest [Sun], and frail elderly for which vaccination is the last push over the edge [Nor].

This report examines causality between observed vaccinations A and mortality B, incorporating repeatability, temporal ordering, random chance and confounders via several known and unknown mechanisms. These include a reverse mechanism from mortality to vaccinations and four mechanisms via infections.

One cannot keep adding possible confounders indefinitely, as that inevitably leads to overmodeling. Every possible confounder exhibits random correlations with both A and B, even unrelated ones such as the weekly number of planet-star eclipses visible from earth. A sufficient number of confounders will swamp any causal effect between A and B at some point. My method

[1] This seems to be the objective of the vague statement when it comes to vaccination and mortality.

includes short-term filtering of all observed data, eliminating *all* confounders that act on a term longer than several weeks, even those unknown, while preventing overmodeling. As collateral damage, the method can only measure causal effects that act on short term and is blind to longer-term effects.

The random weekly variations in infection, vaccination and mortality rates are used as repeated, patterned ocurrences to detect *temporal order* in possible causal directions, while 40+ weeks of data in 2022 are used for statistical *repeatability.* The Bayesian probability framework is used to handle *random chance*.

2.2 Infection-Vaccination-Mortality model

Figure 4 shows my causal infection-vaccination-mortality (IVM) model. Observables are infections, vaccinations and mortality, all weekly absolute numbers in a population. Drivers of the observables are viral waves, campaign dynamics and seasonal baselines. Natural immunity is lifesaving in the real world but not modeled; it acts via a negative feedback loop on infection, whose observations already include the full effect of natural immunity.

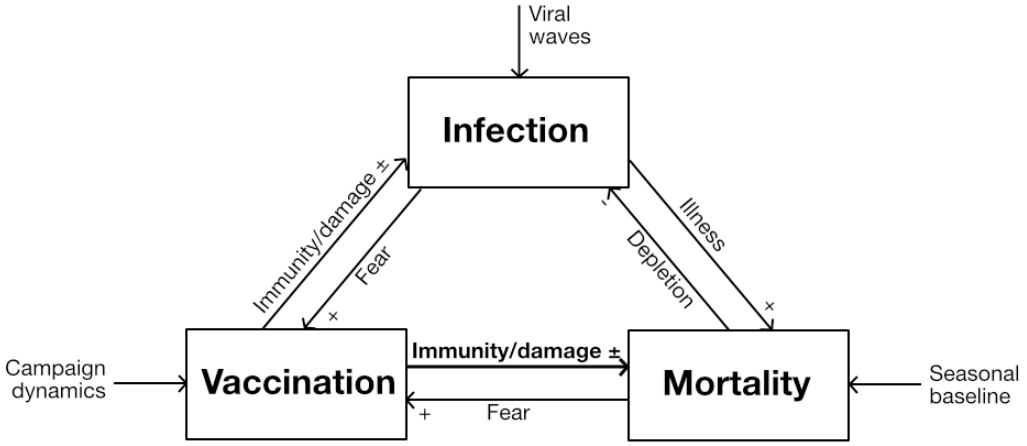

Figure 4: Causal infection-vaccination-mortality (IVM) model. The path of vaccines to mortality has focus. The other five causal paths are confounders. Viral waves, campaign dynamics and seasonal baseline drive the observables and are random sources. As infection data is less reliable, the relative performance of a vaccination-mortality (VM) model without infections and only two causal paths will be evaluated also.

Six directed paths, shown as arrows in Figure 4, model the causal interaction from some event in one observable to events in another observable, either within the same week or in a few future weeks, but not past weeks. Vaccine-induced immunity and damage are modeled together as a single net interaction. Interaction strength is measured in units of a ratio such as mortality per infection (the wellknown Infection Fatality Ratio or IFR), mortality per vaccination (Vaccine Fatality Ratio or VFR), etc.

The focus of this report is measuring VFR via the causal path of vaccination to mortality. The backward confounding path models vaccinations incentivised by fear, caused by observed high excess mortality. Such confounding may add to a positive correlation as in Figure 1, which can easily, but falsely, be attributed to vaccine damage in an analysis that does not take temporal order into account. The four paths connected to infections relate to other confounding mechanisms, among which the depletion of the reservoir of vulnerable people.

2.3 Vaccination-Mortality model without Infections

Infections are the least reliable in the IVM model, not only in terms of data reliability but also by their origin and role in the model. Ideally, two types of infections are taken into account if reliable data is available: *biological* infections which are caused by viral waves and lead to physical illness/death, and *reported* infections that are published by by mass-media with main purpose to induce psychological fear. Two different infection observables, however, strongly increases model dependence on unreliable data, and complexity by number of causal interactions.

I will simply keep one infection observable: the more objective sewer viral particles scaled to equivalent PCR+ tests by calibration in the first part of 2022. The apparent delay in sewer-to-PCR data will be investigated: possibly, compensating the delay may do more harm than good in a causal context.

The IVM model can be used when reliable sewer and/or PCR+ infection data are available. To widen the method's applicability, a simplified model without infections will be introduced: the vaccine-mortality (VM) model, as was effectively used in my prior work [Re2]. The VM model does not suffer from unreliable infection data, but cannot compensate explicitly for infection-based confounders. Its performance will be evaluated relative to the IVM model.

2.4 Bicausal model for data delays

It may happen that observed data include delays due to a variety of reasons, e.g. test-delays until symptoms occur and sewer viral particle data lagging PCR data, see Figure 3. Further, it is common practice to delay vaccination status by several weeks after the "act of vaccination"[2] to account for immunity build-up. Delays are less expected for raw numbers of objectively-dated events as vaccination doses or mortality, but they are still easily introduced e.g. by accident at data transfer to 3rd party data aggregators;, or even purposefully for e.g. visualization or integration of datasets.

Due to unequal delays in observables, temporal ordering may get mixed up and effects may migrate between forward and reverse causal paths in the model, see Figure 5 left. For example, due to a one-week-delay in data, a several-weeks-enduring causal effect in one direction partly migrates to the causal path in opposite direction. This may not be easily identifiable; the migrated part will also change numerically, as paths in opposite directions have inverted units.

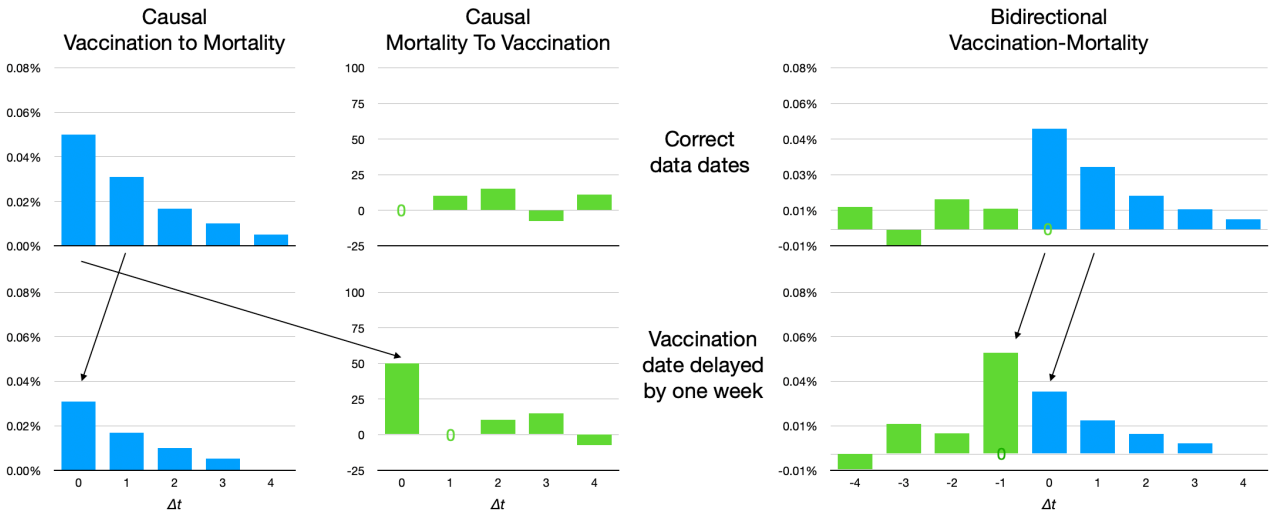

Figure 5: The bicausal model combines two oppositely-directed causal paths into a single bidirectional ("bicausal") path. All data is simulated for illustration purposes. The green zero means a zero effect value.

[2] The clarity of the word "vaccination" has eroded substantially in recent years.

For this reason, I will model every causal path pair as a single *bicausal* path that interacts both backwards and forward in time using one numerical unit, arbitrarily chosen from original forward or backward path. Within a bicausal path, data delays manifest simply as a single shift, see Figure 5 at right. Whenever the forward or backward causal path dominates and activity persists for a few weeks, any delays can be identified by visual interpretation, using common sense aided by strength certainty intervals; I will not try to model/automate such an identification process.

It may appear that the bicausal model causes information loss: in Figure 5, the two causal paths provide 2x5 = 10 measurements, while one bicausal path provides 9 measurements, one less. The two instantaneous parts in the two causal paths at $\Delta t = 0$ get combined into the single instantaneous measurement of the bicausal path. This information loss, although real, is not due to the bicausal model, as in the causal model the instantaneous parts get mixed up too, albeit implicitly. Based on well-known onset latencies of the six causal paths' mechanisms, however, some interactions are zero in the first week (see Figure 5), and all measurements will be uniquely assignable to the six causal mechanisms, both in causal and bicausal model.

2.5 Characteristics of drivers and causal paths

Table 1 shows onset latencies, temporal dynamics, and effect sizes of drivers and causal paths. All effect sizes are very rough estimates by order of ten, and the expected sign of each of the six paths is never used. Measurements will thus never be restricted by a priori sign expectations, but a posteriori inspected for consistency. Free sign modeling is required for vaccine-induced immunity and damage, as they have opposite signs but reside in the same path. Path interaction strengths will be modeled both with prior expectations according to listed effect sizes, and without, that is, completely free of any prior expectation.

Numerically, covid IFR is in the order of 0.1% [Io2]. The VFR is below ~0.1% given that most of the population was vaccinated yearly, baseline mortality is yearly ~1% and total observed excess mortality is in the order of ~10%. Vaccine-Effectivity against infection (VE-I) and mortality (VE-M) may start at ~100% but negative VE-I (positive damage) is known to possibly occur both in the the first weeks during build-up of immunity, and after several months when immunity wears off. The size of vaccine-caused immunity is not plain Vaccine-Effectivity against mortality (VE-M), but scaled by IFR as the paths in my model relate to all-cause mortality instead of only infection-attributed mortality, while assuming that ~100% of the population gets infected each year.

Viral waves, campaign dynamics and seasonal baseline typically evolve on the longer term of months/years, with random variations acting by definition on the shortest term of data resolution, weeks in this report. Vaccine-caused effects have a fast, biological, single-persion underlying mechanism, while mortality-induced fear has a slower, psychological, inter-personal nature, via fear of death induced by observing deaths of others.

For this report, the most essential property in Table 1 is the low onset latency of vaccine damage: adverse systemic events can occur within minutes, with immunity build-up following only in the next 2-4 weeks. The path from infection to death, illness, typically takes at least a week, and slightly above 2 weeks on average [Mar]. The causal path of fear requires data collection, aggregation, and mass-media reporting of high infection numbers, or high excess deaths that are above expectation according to some prognosis. While in 2020 it was custom to broadcast fear-inducing infection and mortality numbers daily, in most of 2022 the number of infections was relatively low, and occurring high excess deaths were not attributable to covid and reported seldom, late, or not at all.

Finally, with depletion the reservoir of vulnerable people more susceptible to mortality declines during periods of excess mortality. Although this effect has zero latency, it acts cumulative and is thus extremely small on the short term, and dynamical, if at all, only on the long term.

Driver	Onset latency	Time scale	Effect size (10-order)
Viral infection waves	-	month	100% population/year
Vaccination campaigns	-	month	100% population/year
Seasonal mortality baseline	-	month	1% population/year
Random fluctations in each	immediate	week*	as observed from data
* zero, limited by source data resolution			
Causal path	**Onset latency**	**Time scale**	**Effect size (10-order)**
Depletion M to I	>> week	months	Negligible < 0.1%
Illness I to M (IFR)	week or more	2 weeks	0.1%
Damage V to M (VFR)	immediate	months	0.1%
Immunity V to M (~VE-M)	2-4 weeks	months	0.1%
Damage V to I (~VE-I)	immediate	2-4 weeks	100%
Immunity V to I (~VE-I)	2-4 weeks	months	100%
Fear I to V	week or more	week	1
Fear M to V	week or more	week	100
IFR: Infection Fatality Ratio, VFR: Vaccine Fatality Ratio VE-I: Vaccine Effectivity against infection, VE-M: against mortality ~ the modeled effects are proportional to VE, and involve additional products with IFR or driver effect size			

Table 1: Time scales, onset latencies and rough order of effect size of drivers and causal paths.

2.6 Confounders

My IVM model handles 5 confounders explicitly, but clearly the list of actual confounders may be longer and full of unknowns. As stated in the causality section, unlimited adding of possible confounders leads to overmodeling. Instead, I will review a few known confounders that may have effect in this model and generic classes of (unknown) confounders.

First, when close-ones (family, friends, neighbours etc) die, shock and mourning may delay planned vaccinations. This path is the same as the fear path, but with opposite/negative sign, not delayed/amplified by mass-media and thus faster/smaller. In most cases, the vaccination will be catched up shortly after, resulting in a slight delay in a few vaccinations. If present, this will be measured as minor initial negative fear, with zero net effect after a few weeks.

Secondly, during vaccination campaigns, typically the smaller group oldest and most vulnerable get vaccinated first, and the broader group of younger and healthier people follow. If vaccinations do cause mortality on the short term, concentrated in older/vulnerable people, the order of vaccinations may create a bias towards “mortality first” followed by “later vaccinations”, a temporal order and positive-signed effect equal to that of the fear path. This confounder makes vaccine damage appear as mortality-induced vaccinations and thus leads to underestimation of vaccine damage, an acceptable bias for VFR measurements.

Many confounders may additionally come into play, known or unknown. All that apply on the long term will be irrelevant, as this study looks only at short-term events, as in Figure 2. Whenever a confounder acts on the short-term, it may reveal itself in both causal directions with similar

strength. In the bicausal measurements in Figure 5, this would appear as a signal without any specific temporal order: evidence of confounding, and absence of causal evidence.

If on the other hand a significant vaccine immunity/damage signal is measured, in absence of a significant fear signal, this is evidence that the signal may not originate from a confounder, and that the measured vaccine effect may be real and causal. Exactly such a signal was found in [Re2]. Of course, it is possible that an unidentifed, short-term causally directed confounder exists. Ignoring alarming evidence by assuming the existence of such a highly characterized but unidentified confounder seems unwise.

2.7 Mathematical representation

Mathematically, I present my model first in full, long-term causal form, and reduce it subsequently to the short-term bicausal model. To start off:

$$\begin{aligned} I(t) &= b_I(t) + r_I(t) + \{V * F_{V\to I}\}(t) + \{M_\Delta * F_{M\to I}\}(t) \\ V(t) &= b_V(t) + r_V(t) + \{I * F_{I\to V}\}(t) + \{M_\Delta * F_{M\to V}\}(t) \\ M(t) &= b_M(t) + r_M(t) + \{I * F_{I\to M}\}(t) + \{V * F_{V\to M}\}(t) \end{aligned} \tag{1}$$

$$\begin{aligned} M_\Delta(t) &= M(t) - M_{expectation}(t) \\ IFR &= \sum_{0\le\Delta t<\Delta T} F_{I\to M}(\Delta t) \\ VFR &= \sum_{0\le\Delta t<\Delta T} F_{V\to M}(\Delta t) \end{aligned} \tag{2}$$

t	Time, integer week number, from $0 \le t < T$
T	Total number of analysed weeks in 2022 (typically $T = 42$ for weeks 9-50)
I, V, M	Weekly number of infections, administered vaccine doses, and all-cause mortality
b_M	Long-term mortality baseline, captures slow variations over months/years
r_M	Short-term weekly variations, uncorrelated zero-mean random process
b_I, r_I, b_V, r_V	Same as mortality baseline, but for viral waves and vaccinations
$*$	Temporal convolution
$F_{A\to B}$	Causal function from A to B, valued only for $0 \le \Delta t < \Delta T$
ΔT	Duration of short-term causal effect (typically $\Delta T = 2..5$ weeks)
$M_{expectation}$	Some prognosis, expected mortality, slowly varying over time (seasonal)
M_Δ	Excess mortality with respect to the prognosis/expectation
IFR	Infection Fatality Ratio, total mortality caused by infection
VFR	Vaccine Fatality Ratio, total mortality caused by vaccination

The b_I, b_V, b_M and r_I, r_V, r_M are the drivers. The "baselines" b_I, b_V, b_M vary slowly on the longer-term of a month/year. They capture viral presence waves, overall vaccination campaign dynamics, and mortality of seasonal waves, other-cause waves (covid, NPIs). They also capture confounders acting between them, on the long-term, such as vaccination campaigns planned during covid waves. The r_I, r_V, r_M random processes describe the spread around the baselines, or weekly variability of infections, vaccination and mortality originating from chance. They are zero-mean

and uncorrelated over time and with respect to eachother, and non-stationary with variance changing slowly over the longer-term together with b_I, b_V, b_M.

The six $F_{A\to B}$ causal functions model the six causal paths in Figure 4, with main focus on $F_{V\to M}$. All $F_{A\to B}$ operate by temporal convolution, a linear operator. The linearity of $F_{V\to M}$ is particularly justifed, as individual biological mechanisms within a population have no direct causal interaction that could lead to substantial nonlinearities. For fear paths $F_{M\to V}$ and $F_{I\to V}$, linearity may be less defendable as the underlying psychological mechanism may involve nonlinear effects, e.g. "100 deaths" causing double the fear of "99 deaths". For immunity path $F_{V\to I}$, and possibly $F_{V\to M}$, one can argue that these should include a product with viral presence/infections I, but this is not taken into account for mathematical simplicity. An argument that justifies this choice partly is that covid has become endemic and viral waves are less extreme. Also, other pathogens provide a permanent infectious background and it makes sense to evaluate vaccine effectivity always and only against all-cause mortality [Ben]; ideally infections I would represent all pathogens, or even other mortal threats[3]. Altogether, modeling of $F_{V\to M}$ and VFR may thus be more accurate than the other paths, which is acceptable regarding the aim of this report.

The mortality to vaccination and infection functions $F_{M\to V}$,$F_{M\to I}$ have M_Δ as argument; fear and depletion are caused by excess mortality or above-expectation mortality $M - M_{expected}$. There are other ways expectations may impact $F_{M\to V}$, e.g. when a newer expectation is published that overshadows an older expectation, the newer creates additional fear and it may thus appear with a positive sign: $M_{newer\ expectation} - M_{older\ expectation}$. For this analysis, it is irrelevant how and when expectations are constructed, whether or not they include the effects of covid, NPIs, whether calculated by a national institute or emerged within the minds of individuals, whether their effect sign is positive or negative. What is important, is that expectations change slowly over time t, and that the sign of actual, observed mortality M is always positive in M_Δ.

2.8 Short-term filter

As in [Re2], I apply a linear temporal filter $W(\Delta t)$ on source data I, V, M to remove all long-term events and extract short-term events in $\hat{I}, \hat{V}, \hat{M}$ (with a hat), see also Figure 6:

$$\begin{aligned} W(\Delta t) &= [-0.05\ -0.25\ +0.6\ -0.25\ -0.05] \quad \text{for } \Delta t \in [-2,2] \\ \hat{I}(t) &= \{W * I\}(t) \\ \hat{V}(t) &= \{W * V\}(t) \\ \hat{M}(t) &= \{W * M\}(t) \end{aligned} \tag{3}$$

Applied to (1), this results in:

$$\begin{aligned} \hat{I}(t) &= \hat{r}_I(t) + \{\hat{M} * F_{M\to I}\}(t) + \{\hat{V} * F_{V\to I}\}(t) \\ \hat{V}(t) &= \hat{r}_V(t) + \{\hat{M} * F_{M\to V}\}(t) + \{\hat{I} * F_{I\to V}\}(t) \\ \hat{M}(t) &= \hat{r}_M(t) + \{\hat{I} * F_{I\to M}\}(t) + \{\hat{V} * F_{V\to M}\}(t) \end{aligned} \tag{4}$$

[3] Mass-media have suggested vaccination protects against car crashes.

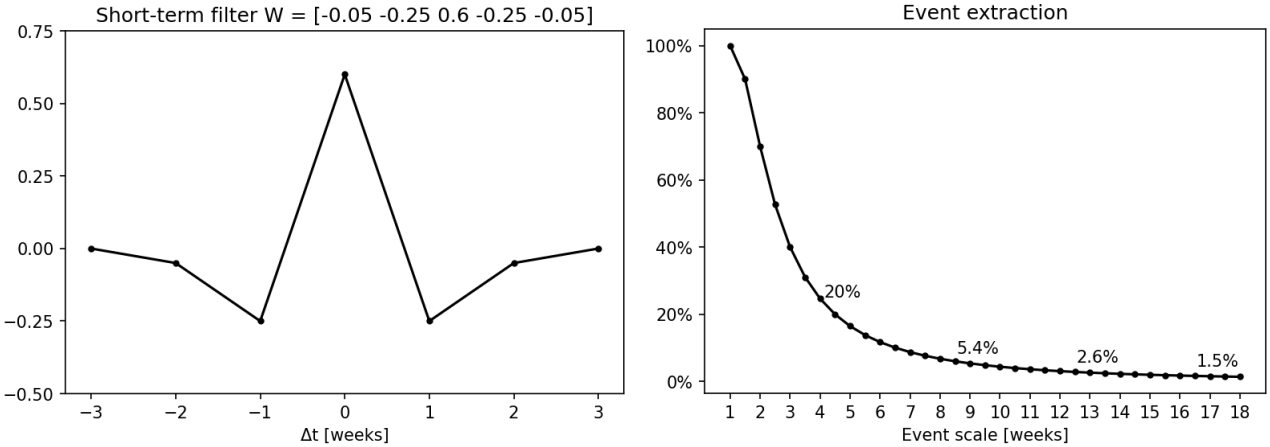

Figure 6: The temporal filter W extracts events with a short temporal scale, and removes events with longer temporal scale.

Importantly, all causal functions $F_{A\to B}$ are *unaffected* by the short-term filter, and subsequently so is VFR in (2). The short-time versions of source data $\hat{I}(t), \hat{V}(t), \hat{M}(t)$ are *zero-mean* random variables, illustrated by Figure 2. All long-term baselines b_I, b_V, b_M and mortality expectation $M_{expectation}$ have disappeared, also causing excess mortality M_Δ in (1) to be replaced by plain short-term filtered mortality $\hat{M}$ in (4). The filtered versions of drivers $\hat{r}_I(t), \hat{r}_V(t), \hat{r}_M(t)$ have slightly reduced variance compared to the unfiltered signals, and are still non-stationary.

All of this is irrespective of the specific choice of filter W, as long as it extracts short-term events as in Figure 6. The filter choice (3) in this report is given by $W(\Delta t) \approx \delta(\Delta t) - KG_1(\Delta t)$, where δ is a Dirac delta function, G_σ is a zero-mean, σ-deviation Gaussian, one of the smoothest filters possible, and K is chosen to ensure that W is zero-mean (sum coefficients is zero). The filter choice in [Re2], $[-0.1\ -0.25\ +0.7\ -0.25\ -0.1]$, was an intuitive approximation of the filter in this report.

As the same filter is applied to all observables, it does not bias the short-term measurements towards any of the causal paths, or towards any direction within any path; the filter may even be time-assymetric, e.g. a 3rd derivative filter [-1 +3 -3 +1], as possible time delays due to the filter do not affect measurements of $F_{A\to B}$. The filter also does not bias measurements by sign. In combination with zero-mean prior expectations on the values of $F_{A\to B}$, the filter may bias measurements towards zero, with a relative strength growing with event time scale. Aggregates of $F_{A\to B}$ such as IFR and VFR will then be biased to zero, or equivalently underestimated in size.

In the results section, I will illustrate a few alternative filters as well as absence of the filter, and complete relaxation of the prior expectations. For readability: ***I will leave out all hats from this point on.*** In all that follows, observables I, V, M are short-term-filtered.

2.9 Short-term causal IVM model, prior variances and constraints

The short-term causal IVM model (4) is here denoted without hats:

$$\begin{aligned} I(t) &= r_I(t) + \{M * F_{M\to I}\}(t) + \{V * F_{V\to I}\}(t) \\ V(t) &= r_V(t) + \{M * F_{M\to V}\}(t) + \{I * F_{I\to V}\}(t) \\ M(t) &= r_M(t) + \{I * F_{I\to M}\}(t) + \{V * F_{V\to M}\}(t) \end{aligned} \tag{5}$$

I model all t and Δt components of drivers r_I, r_V, r_M and causal interactions $F_{A\to B}$ as independent, normal-distributed (Gaussian) stationary random variables. The original non-stationarity of drivers r_I, r_V, r_M is remodeled by a slightly higher overall variance, namely that of the observed I, V, M:

$$\sigma_{r_I} = \sigma_I \qquad \sigma_{r_V} = \sigma_V \qquad \sigma_{r_M} = \sigma_M \tag{6}$$

For the $F_{A\to B}$ variances one finds using the effect sizes in Table 1:

$$\begin{aligned} &\sigma_{V\to M} = 10^{-3} \qquad \sigma_{M\to I} = 10^{-3} \qquad \sigma_{I\to V} = 1 \\ &\sigma_{M\to V} = 10^{2} \qquad \sigma_{I\to M} = 10^{-3} \qquad \sigma_{V\to I} = 1 \end{aligned} \tag{7}$$

These values are rough orders, which is accurate enough as they are only used as so-called "priors" to slightly constrain the model; they bias measurements of $F_{A\to B}$ to zero in the presence of insufficient evidence in the observables. The priors' influence decreases the more informative observational data I, V, M is available. I will alternatively allow for completely free causal interactions, relaxing prior variance constraints (7), to prevent underestimation of interactions $F_{A\to B}$:

$$\sigma_{A\to B} = \infty \tag{8}$$

Using Table 1 one finds that fear and depletion causal paths have onset latencies beyond a week:

$$F_{I\to V}(0) = F_{M\to V}(0) = F_{M\to I}(0) = 0 \tag{9}$$

Although the illness path, death caused by infection $F_{I\to M}$, also has an onset latency of a week, I choose not to take it into account explicitly as a prior restriction. The three restrictions (9) already suffice to disambiguate bicausal interactions at $\Delta t = 0$, and it is plausible that a highly vulnerable person dies within a week after infection due to illness caused.

2.10 Time resolution and onset latency

Figure 7 illustrates how finite temporal data resolution affects observations and causal functions F. The underlying (inaccessible) time-continuous causal mechanism F^c (with upper c) translates to week resolution by a specific triangular-shaped time-symmetric aggregation filter Λ:

$$F(\Delta t) = \{F^c * \Lambda\}(\Delta t) = \int_{\Delta t^c} F^c(\Delta t^c)\Lambda(\Delta t - \Delta t^c)d\Delta t^c \tag{10}$$

with t^c continuous (real-valued) time in weeks. The triangular aggregation effect happens always, no matter how fine the time resolution used. The week-resolution used in this report means that any event pair separated by 3.5 days or more, is thus captured more by $F(1)$ than $F(0)$.

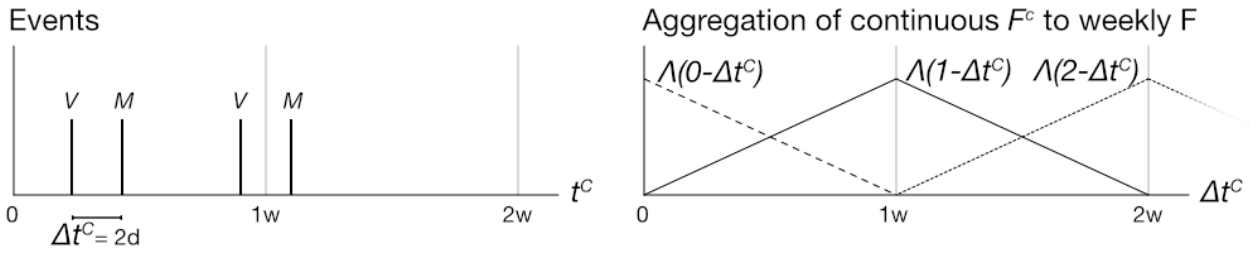

Figure 7: Resolution effect example for vaccination to mortality. Event pairs separated by 2 days are captured by $F_{V\to M}(0)$ and $F_{V\to M}(1)$, randomly with probability 5/7 and 2/7 respectively, depending on location of events within the week. The amounts are described by triangular function Λ of separation duration.

Most important for this report, any event pair separated by a week or more will under no circumstance affect $F(0)$, justifying the onset latency constraints (9).

2.11 Bicausal IVM and simplifed VM model

The bicausal IVM model combines the causal model's six paths as in Figure 4 into three bicausal paths, by new functions $F_{A\leftrightarrow B}$ (note the double arrow):

$$F_{A\leftrightarrow B}(\Delta t) = F_{A\to B}(\Delta t) + \frac{\sigma_B^2}{\sigma_A^2} F_{B\to A}(-\Delta t) \qquad , \; -\Delta T < \Delta t < \Delta T \tag{11}$$

Each $F_{A\leftrightarrow B}$ will be measured and is subsequently uniquely decomposable into $F_{A\to B}$ and $F_{B\to A}$, as the latter are both only valued for $\Delta t \geq 0$. Ambiguities at $\Delta t = 0$ are completely resolved by onset latency constraints (9). The scale of $F_{A\leftrightarrow B}$ has the same scale as $F_{A\to B}$ namely B per A, and thus $F_{B\to A}$'s scale of A per B is corrected for in (11). Note that the $F_{B\to A}$ in (11) models the exact same physical event as in (5), with same accuracy, but with a slightly different mathematical representation. Under expected circumstances where causal path effects are relatively small compared to the drivers, the difference is negligibly small.

The combined functions can be chosen as $F_{A\leftrightarrow B}$ or $F_{B\leftrightarrow A}$ for each of the three path pairs in causal model (5). I choose them to match the biological causal paths, at the same time arriving at only two equations:

$$\begin{aligned} M(t) &= r_M(t) + \{V * F_{V\leftrightarrow M}\}(t) + \{I * F_{I\leftrightarrow M}\}(t) \\ I(t) &= r_I(t) \; + \{V * F_{V\leftrightarrow I}\}\;(t) \end{aligned} \tag{12}$$

Variances (7) combine via (11) into:

$$\sigma_{V\leftrightarrow M} = 10^{-3} \qquad \sigma_{I\leftrightarrow M} = 10^{-3} \qquad \sigma_{V\leftrightarrow I} = 1 \tag{13}$$

From here, the simplified bicausal VM model without infections is:

$$M(t) = r_M(t) + \{V * F_{V\leftrightarrow M}\}(t) \tag{14}$$

with only one prior $\sigma_{V\leftrightarrow M}$ from (13). In [Re2], $F_{V\leftrightarrow M}$ of this bicausal VM model was estimated by a Pearson correlation trend factor:

$$F_{V\leftrightarrow M}(\Delta t)_{[Re2]} \approx \frac{COV\big(V(t), M(t+\Delta t)\big)}{VAR\big(V(t)\big)} \tag{15}$$

This estimate was sub-optimal; next follows an optimal estimation procedure.

2.12 Bayesian probabilities and estimating parameters

The Bayesian probability framework is an ideal, systematic tool to obtain conditional probability densities $P_{F|I,V,M}$ of model parameters F given observed I, V, M. From the $P_{F|I,V,M}$ relevant statistics as mean and variance of F can be extracted. Denoting all drivers by $r = \{r_I, r_V, r_M\}$, one obtains for the causal IVM model $F = \{F_{V\to I}, F_{I\to V}, F_{I\to M}, F_{M\to I}, F_{M\to V}, F_{V\to M}\}$:

$$\begin{aligned}
P_{F|I,V,M} &= \int_r P_{r,F|I,V,M} = \int_r P_{I,V,M|r,F} P_{r,F} P^{-1}_{I,V,M} = P^{-1}_{I,V,M} P_F \int_r P_r P_{I,V,M|r,F} \\
&= P^{-1}_{I,V,M} \prod_{F_{A\to B}\in F} \prod_{\Delta t} G_{\sigma_{A\to B}}\big(F_{A\to B}(\Delta t)\big) \\
&\quad \int_{r_I,r_V,r_M} \prod_t G_{\sigma_I}\big(r_I(t)\big)\cdot G_{\sigma_V}\big(r_V(t)\big)\cdot G_{\sigma_M}\big(r_M(t)\big)\cdot \\
&\quad \det \mathbf{J}(F)\cdot \delta\left(I(t) - r_I(t) - \{V\ * F_{V\to I}\}(t) - \{M * F_{M\to I}\}(t)\right)\cdot \\
&\quad \delta\left(V(t) - r_V(t) - \{M * F_{M\to V}\}(t) - \{I * F_{I\to V}\}(t)\right)\cdot \\
&\quad \delta\left(M(t) - r_M(t) - \{I * F_{I\to M}\}(t) - \{V * F_{V\to M}\}(t)\right)\cdot \\
&= K \prod_{F_{A\to B}\in F} \prod_{\Delta t} G_{\sigma_{A\to B}}\big(F_{A\to B}(\Delta t)\big)\cdot \\
&\quad \prod_t G_{\sigma_I}\big(I(t) - \{V * F_{V\to I}\}(t) - \{M * F_{M\to I}\}(t)\big)\cdot \\
&\quad\quad G_{\sigma_V}\big(V(t) - \{M * F_{M\to V}\}(t) - \{I * F_{I\to V}\}(t)\big)\cdot \\
&\quad\quad G_{\sigma_M}\big(M(t) - \{V * F_{V\to M}\}(t) - \{I * F_{I\to M}\}(t)\big) \\
&= G_{\mu,\Sigma}(F) \sim e^{-\frac{1}{2}\{(F-\mu)^\dagger \boldsymbol{\Sigma}^{-1}(F-\mu)\}}
\end{aligned} \tag{16}$$

First row: the intermediate roles of drivers r are taken into account via integrals, and observations and model parameters are reversed bringing up additional priors, of which the model parameters P_F are independent. Second row: prior P_F is expanded in 6 causal paths $F_{A\to B}$ and all Δt components. Row 3: prior P_r is split in individual drivers and time $0 \le t < T$. Rows 4-6: causal IVM model (5) enters via three Dirac δ functions plus so-called determinant of Jacobian $\mathbf{J}$ that describes the multiple occurences of I, V, M in the δ arguments. The Jacobian $\mathbf{J}$ is a huge $3T$-by-

$3T$ matrix full of zeros, ones, and (minus the) values of all 6 causal paths $F_{A\to B}$. Luckily, this determinant can be computed analytically:

$$\begin{aligned}\det \mathbf{J}(F) = \{1 &- F_{M\to V}(0)F_{V\to M}(0) - F_{I\to V}(0)F_{V\to I}(0) - F_{I\to M}(0)F_{M\to I}(0) \\ &-F_{I\to M}(0)F_{M\to V}(0)F_{V\to I}(0) - F_{I\to V}(0)F_{V\to M}(0)F_{M\to I}(0) \quad \}^T \\ &= 1\end{aligned} \tag{17}$$

where the 2nd equality is due to onset latency constraints (9). At the 3rd equality in (16), the determinant is gone, prior $P^{-1}_{I,V,M}$'s value is unknown and replaced by constant K; the prior is constant as I, V, M are fixed, observed source data. Also, the integrals transfer the causal model from the δ functions to the priors of the drivers r. As the final result contains only Gaussians and a constant, it must be a simple multivariate Gaussian distribution $G_{\mu,\mathbf{\Sigma}}(F)$ with mean μ and covariance matrix $\mathbf{\Sigma}$ as in the final row.

For the bicausal IVM and VM models, $\det \mathbf{J}(F)$ is also 1 and a similar multivariate Gaussian is obtained. Mean and variance of F's single components or linear combinations such as VFR can be obtained analytically. For example, one finds for the bicausal VM model a so-called least-squares/minimum-norm solution (with $\Delta T = 3$ for clarity):

$$\mathbf{V} = \begin{bmatrix} V(2) & V(1) & V(0) & 0 & 0 \\ V(3) & V(2) & V(1) & V(0) & 0 \\ V(4) & V(3) & V(2) & V(1) & V(0) \\ & & \vdots & & \\ V(T-2) & V(T-3) & V(T-4) & V(T-5) & V(T-6) \\ V(T-1) & V(T-2) & V(T-3) & V(T-4) & V(T-5) \\ 0 & V(T-1) & V(T-2) & V(T-3) & V(T-4) \\ 0 & 0 & V(T-1) & V(T-2) & V(T-3) \end{bmatrix}, \; O = \begin{bmatrix} 0 \\ 0 \\ 1 \\ 1 \\ 1 \end{bmatrix}$$

$$\begin{aligned} \mathbf{\Sigma} &= (\sigma_M^{-2}\mathbf{V}^\dagger\mathbf{V} + \sigma_{V\leftrightarrow M}^{-2}\mathbf{I})^{-1} \\ \mu &= \mathbf{\Sigma}\sigma_M^{-2}\mathbf{V}^\dagger M \\ F_{V\leftrightarrow M} &= \mu \quad \pm \text{ diag}(\mathbf{\Sigma})^{\frac{1}{2}} \\ VFR &= O^\dagger\mu \; \pm \; (O^\dagger\mathbf{\Sigma}O)^{\frac{1}{2}} \end{aligned} \tag{18}$$

where $\mathbf{I}$ is the identity matrix, $\dagger$ is matrix transpose, and $\pm$ separates mean and standard deviation. If the prior variance on $F_{V\leftrightarrow M}$ is completely relaxed ($\sigma_{V\leftrightarrow M} = \infty$), one gets the so-called least-squares solution:

$$\begin{aligned} \mu &= (\mathbf{V}^\dagger\mathbf{V})^{-1}\mathbf{V}^\dagger M \\ \mathbf{\Sigma} &= (\mathbf{V}^\dagger\mathbf{V})^{-1}\sigma_M^2 \end{aligned} \tag{19}$$

Bayesian approaches are ideal to obtain probabilistic answers to hard, binary questions such as whether "vaccination has a net mortal effect in the first few weeks" (hypothesis H_{mortal}), or not ($\bar{H}_{mortal}$). With VFR mean and variance from (18), one finds:

$$\Pr\{H_{mortal}\} = \Pr\{VFR > 0\} = \frac{1}{2} + \frac{1}{2}\text{erf}(\frac{\mu_{VFR}}{\sqrt{2}\sigma_{VFR}}) \tag{20}$$

This is a true probability, not a so-called likelihood ratio between two hypotheses: As the set of hypotheses $\{H_{mortal}, \bar{H}_{mortal}\}$ is complete in all possible outcomes, there are no other (unknown) competing hypotheses possible.

Any prior belief in any of the two hypotheses has already been accounted for in the calculation of VFR. If one has a strong prior belief in $\bar{H}_{mortal}$, one should incorporate this by a negative-mean expectation of $F_{V\to M}$ in *the first few weeks*, which is counter to commonly accepted knowledge that protective effects of vaccines do not occur in the first few weeks. Logically, one cannot first accept the computation of VFR, and subsequently reject (20) on the basis that it does not incorporate an additional explicit prior biasing towards $\bar{H}_{mortal}$ reflecting one's beliefs.

3 Results

I apply the bicausal model to booster campaigns during 2022 in The Netherlands (population ~18M). Infection, vaccination and mortality data are unstratified, weekly, total absolute numbers from public national sources [Src]. With PCR+ and sewer viral-particle-based infection data available, the IVM model is used to determine the usability of sewer data and relevance of infection confounders, all compared to the relative performance of the infection-less VM model. With the VM model, a few additional experiments are performed with different short-term filters and periods, mortality age groups, and relaxation of prior variances on causal interactions F.

Finally, I apply the bicausal VM model to 30 European countries (~530M people) with data from aggregation sources [Eur, Owi] in 2022 during weeks 10-43 (limited by data availability).

3.1 Sewer data for infections in the IVM model

Sewer viral particle data are publicly available for The Netherlands, see Figure 3. In weeks 1-20 of 2022, PCR tests were performed in higher volumes; I use this period to compute a scale constant of PCR+ tests per sewer viral particle, and convert the more objective sewer data over entire 2022 to PCR-equivalent infections I.

Figure 8 shows results of the bicausal IVM model, with PCR and sewer infection data, weeks 9-50 during the vaccination campaigns. Although few measurements are significant, a few observations can be made. PCR-based infection-to-mortality suggests a peak at $F_{I\to M}(2)$, matching the expected average time from infection to death. The sewer-based curve peaks just significantly at $F_{I\to M}(0)$, suggesting sewer-based measurements lag by a two-week time delay. Applying a minus-two-week-shift in sewer data to compensate the delay brings the sewer-based infection-to-mortality peak also at $F_{I\to M}(2)$.

The individual PCR-based vaccination-to-mortality measurements of $F_{V\to I}$ and 5-week-net-result -9±7% after vaccination are just significant, and the probability that the vaccine protects against infection (hypothesis $H-$) is 91%. The original unshifted sewer-based measurements suggest that vaccination *causes* infections with a probability 83%. The 2-weeks shifted sewer

measurements solve this uncomfortable finding, but bring up a logical, causal issue: the shift brings the peak towards $F_{I\to V}(1)$, infection-induced-vaccinations via fear. This is, however, not causally possible as the original unshifted sewer data cannot cause fear *before* being measured. As can be seen in Figure 3, PCR+ testing was quite low for most of 2022, and its media-reporting seem unable to have simultaneously produced the same required fear, as is also visible in Figure 8 by $F_{I\to V}$ with 5-week-net-result -0.53±2.67.

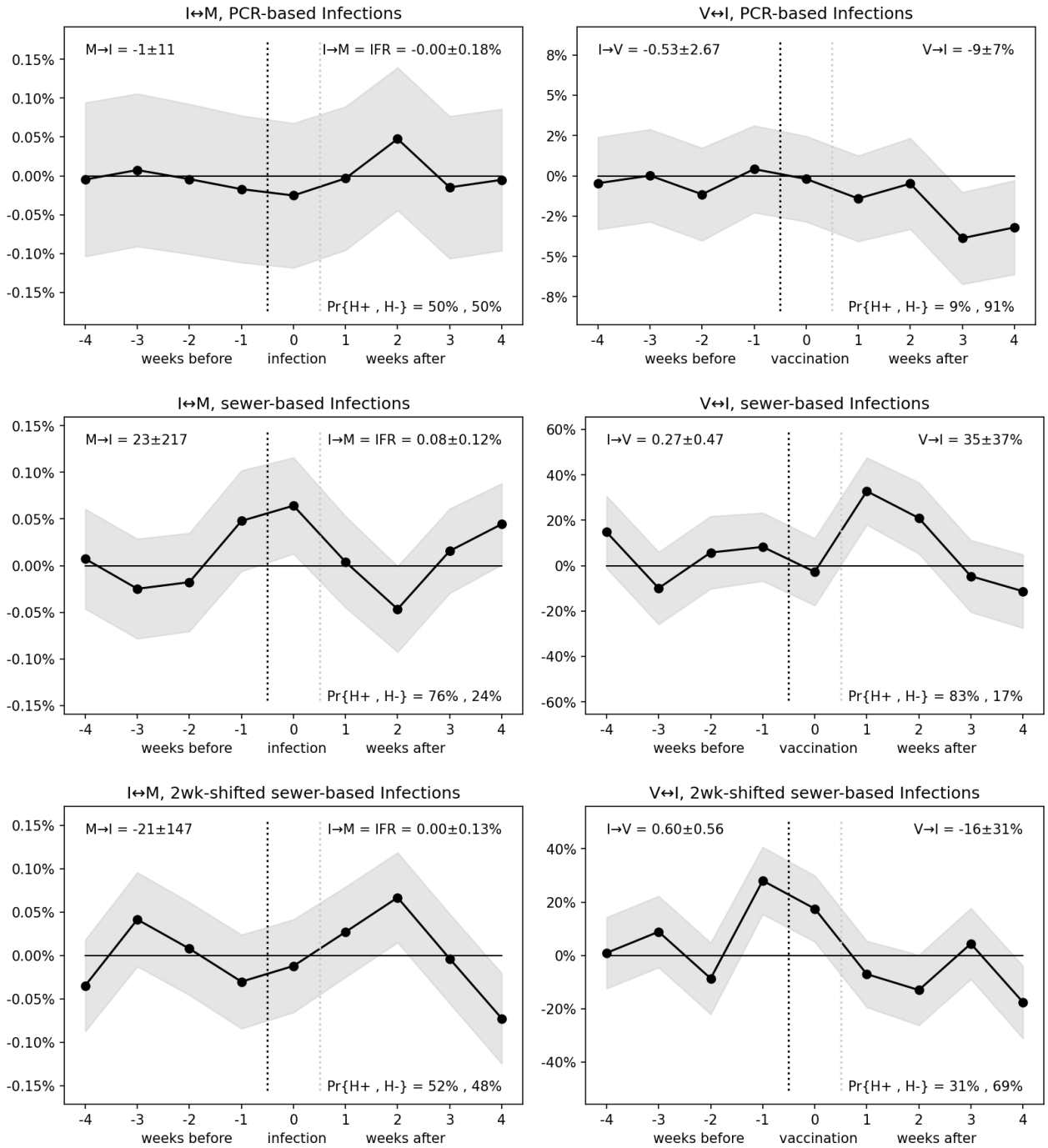

Figure 8: Results for bicausal IVM model, infection-mortality and vaccination-mortality interactions, with PCR+ and sewer measurements, weeks 9-50 of 2022 in The Netherlands. Black dotted lines indicate week $\Delta t = 0$ is assigned to right, biological causal path according to onset latencies. Y-axis has biological path scale. Grey areas indicate ±1 sigma interval. Pr indicates Bayesian probability of the biological path to be net positive or negative (hypotheses $H+$ and $H-$).

These results suggest that sewer data should not be back-shifted in time, and that the *viral particles in the sewer are caused by vaccination*. The possibility that sewer data is measuring spike (S) particles created directly by vaccinations can be excluded, as there is no overlap between viral genes used for sewer measurements (N/E) and vaccination (S) [Med]. Recent research did find evidence that infections correlate strongly with vaccinations [Shr].

Using $\Delta T = 5$, a PCR-equivalent ratio of infections/reactivations per vaccination is found as just-not-significant 0.35±0.37, see Figure 8 right-center. Figure 9 shows the same result with $\Delta T = 3$: with more than 99% probability, vaccination causes viral particles to increase ($H+$) in the first three weeks since vaccination. The amount of equivalent-PCR-infections per vaccination is 0.50±0.21 (95% CI 0.08-0.92). This number is very high; possibly the equivalent PCR+/sewer-particle scale factor is not well estimated or applicable. An additional explanation is that besides triggering infections, vaccinations may reactivate latent viral (particle) reservoirs.

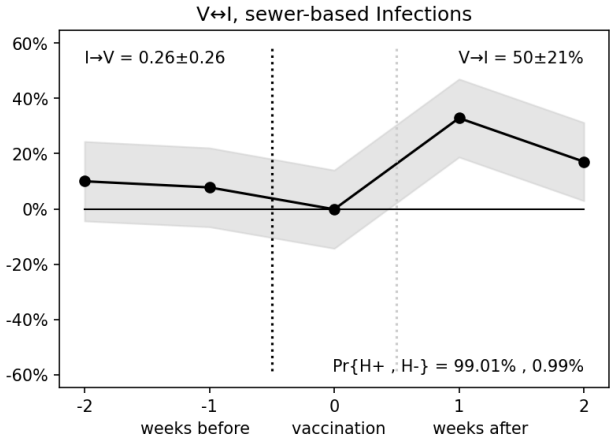

Figure 9: The causal effect of vaccinations on infections as measured effectively by sewer viral particles.

3.2 IVM versus VM model

Figure 10 shows $F_{V\to M}$ and VFR obtained via the IVM model via PCR+, plain and 2-weeks-backshifted sewer-based infections, and the VM model without infections, in weeks 9-50 in The Netherlands. In all four cases a causal temporal order effect can clearly be seen, with mortality insignificant before vaccination and significant after. Also in all four cases, $F_{V\to M}(0)$ equals 0.09±0.03%, that is, vaccine-induced mortality in the same week of vaccination is near 0.1%, with 3-sigma confidence. Finally, again in all 4 cases, VFR over 5 weeks is just insignificant at ca 0.07±0.09%.

Apparently, infections did not confound mortality and vaccination in The Netherlands in 2022, in a significant way measurable by the IVM model. Based on these results, I conclude that the IVM model does not offer substantially different or better results compared to the simpler VM model without infection confounders.

The insignificance of VFR appears caused by a negative $F_{V\to M}$ after two weeks and an increasing sigma when aggregating $F_{V\to M}$ over $\Delta T = 5$ weeks. The positive-negative-dynamics of $F_{V\to M}$ are consistent with vaccination being the last push to mortality for highly vulnerable people. The probability that vaccination causes net mortality over the entire 5 weeks after vaccination ($H+$) remains however ca 75%-80% in all cases. The VFR found is lower but order-comparable to that of my prior work [Re2], which found ~0.18% in weeks 9-34 of 2022, using age-correction in vaccination-mortality data, and a suboptimal estimation procedure.

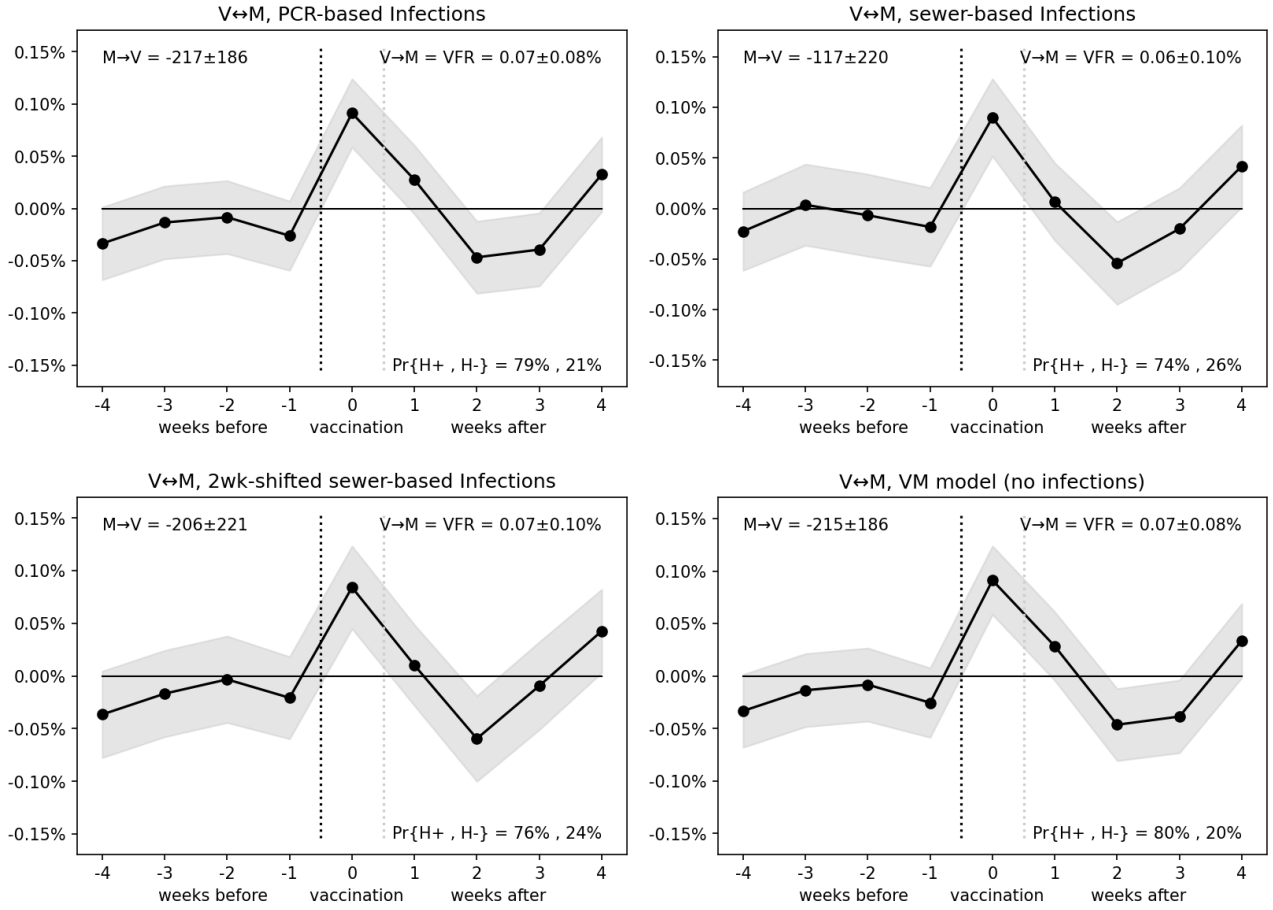

Figure 10: Results for $F_{V\to M}$ and VFR with bicausal IVM and VM models, with and without infection confounder, weeks 9-50, The Netherlands.

3.3 Short-term filter, period, relaxation of prior, age groups

Table 2 shows VFR using the VM model, for different short-term periods ΔT, filters W and relaxation of prior variance $\sigma_{V\to M} = \infty$. It shows that shorter ΔT periods lead to better/lower result variances, and that varying filter W has marginal influence. Most importantly, relaxing the prior from zero-mean Gaussian with $\sigma_{V\to M} = 10^{-3}$ to a uniform unbiased prior with $\sigma_{V\to M} = \infty$ has no significant influence.

Figure 11 illustrates a few results: the significant result with $\Delta T = 2$ without prior, an isolated central peak in $F_{V\to M}$ with $\Delta T = 16$, and the erratic effect of not using any short-term filter. Figure 12 shows a result for age groups: significant $F_{V\to M}$ is concentrated at ages 65+.

	$\Delta T = 2$	$\Delta T = 3$	$\Delta T = 5$
default VM model	0.12±0.04% (99.9%)	0.09±0.05% (97%)	0.07±0.08% (80%)
Relaxed prior $\sigma_{V\to M} = \infty$	0.13±0.04% (99.9%)	0.10±0.05% (98%)	0.07±0.09% (79%)
W = [-0.25 +0.5 -0.25]	0.14±0.04% (99.9%)	0.11±0.05% (97%)	0.07±0.09% (80%)
W = [-1 +3 -3 +1]	0.14±0.07% (97.7%)	0.13±0.10% (89%)	0.06±0.16% (66%)

Table 2: VFR and ($Pr\{VFR \geq 0\}$) with bicausal VM model for several different short-term periods, filters, and relaxation of prior variance.

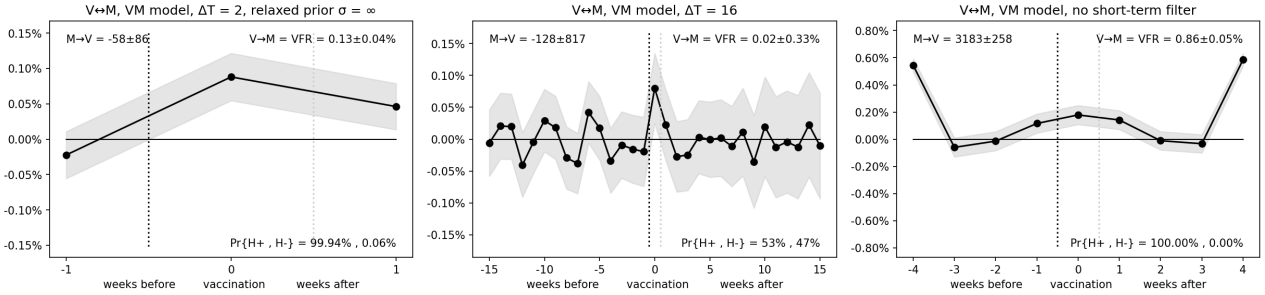

Figure 11: A few results with short-term periods $\Delta T = 2$, $\Delta T = 16$ and without short-term filter.

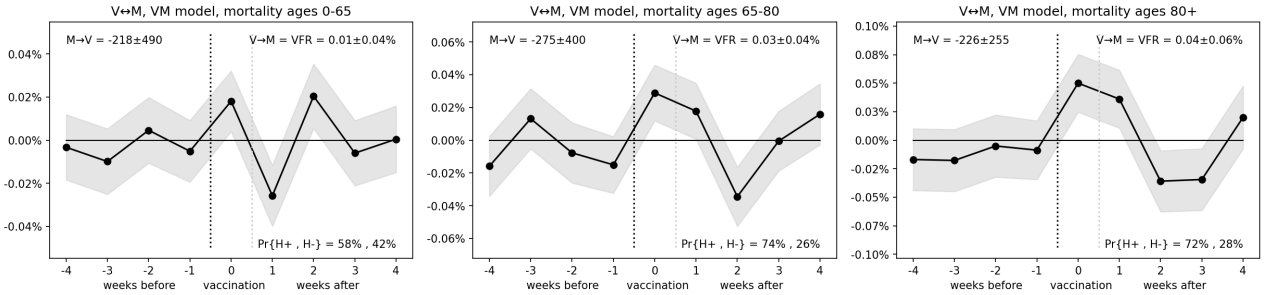

Figure 12: Results with bicausal VM model for several age groups (mortality data age-stratified, vaccination data is all-ages). VFR is concentrated at ages 65+.

3.4 Europe

I applied the bicausal VM model on 30 European countries using data from aggregators [Eur,Owi] in weeks 10-43. Countries include Austria, Belgium, Bulgaria, Croatia, Czechia, Denmark, Estonia, Finland, France, Germany, Greece, Hungary, Iceland, Italy, Latvia, Liechtenstein, Lithuania, Luxembourg, Malta, Netherlands, Norway, Poland, Portugal, Romania, Slovakia, Slovenia, Spain, Sweden, Switzerland and United Kingdom.

Figure 13 shows results for The Netherlands, with data from the same national source used in previous sections and the aggregation sources. Clearly, aggregator data has been processed. This may involve smoothing or small accidental/deliberate data shifts in time, e.g. to align data sets or optimize visualization for their online services. In this study, however, it negatively affects the significance of measurements.

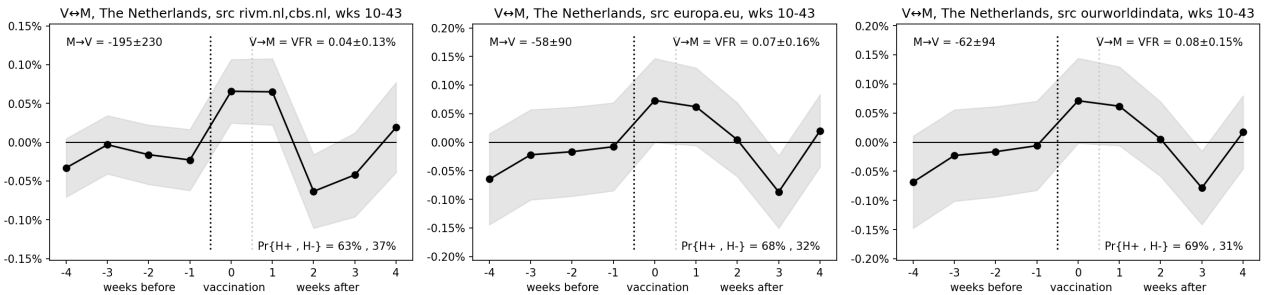

Figure 13: Results with bicausal VM model for The Netherlands, weeks 10-43, data from three different sources [Src,Eur,Owi].

Figure 14 shows results for a selection of European countries. Clearly, the individual results lack significance.

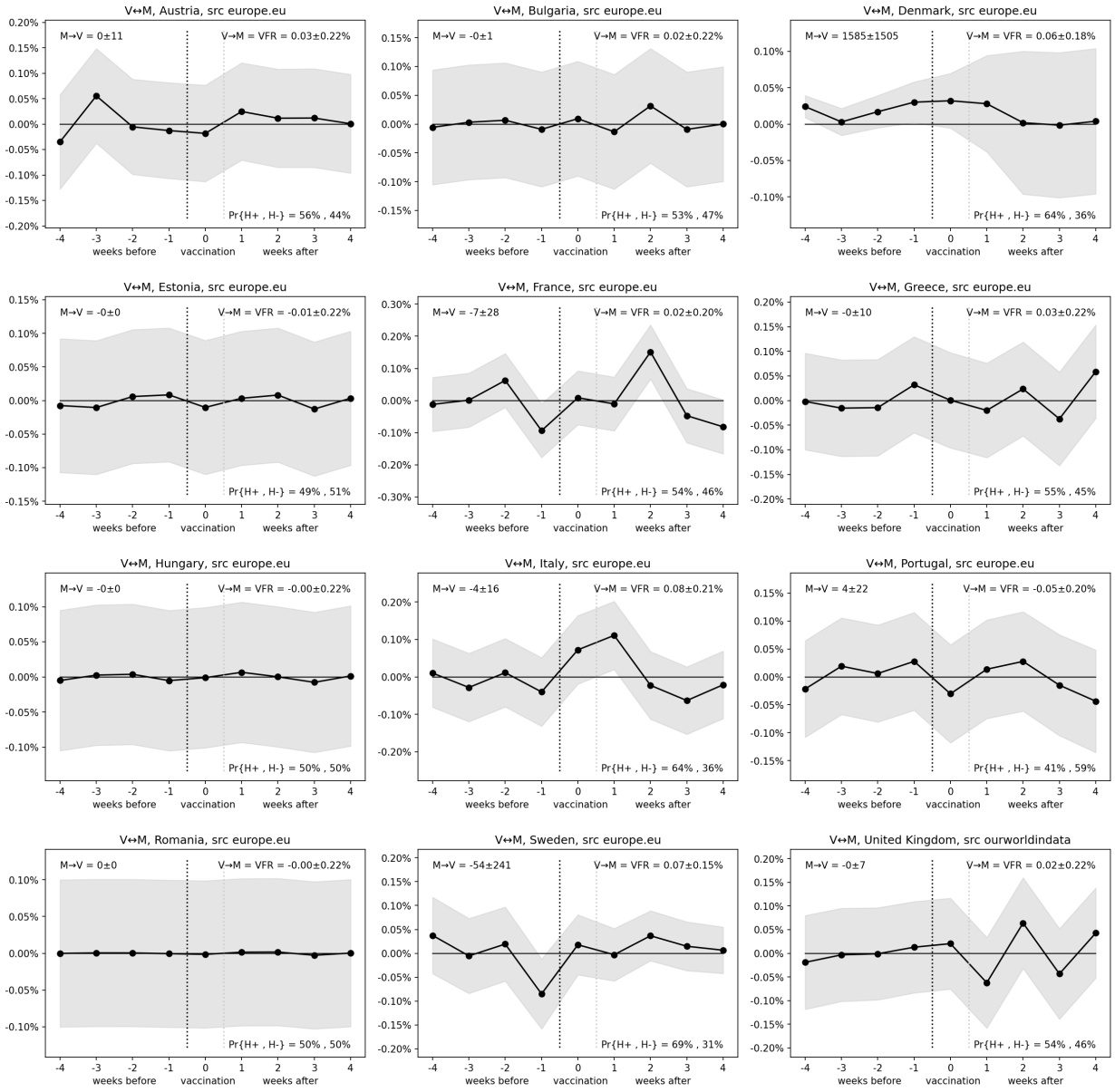

Figure 14: Results for several individual countries, weeks 10-43 (data from [Eur], UK data was available only at [Owi]).

Significant results are obtained when data from all 30 countries are combined. Table 3 shows results for $\Delta T = 3$, with/without relaxation of prior expectations. Figure 15 shows a result with $\Delta T = 5$: all $F_{V \to M}$ are significantly different from zero, and all $F_{M \to V}$ are not, evidence for a significant mortality effect caused by vaccination, not involving a confounder. In absence of any prior expectation, a VFR of 0.35% ±0.10% is obtained according to Table 3 in the first 3 weeks.

Prior model variance $\sigma_{V \to M}$	Data source [Eur]	Data source [Owi]
10^{-3}	0.26±0.08% (99.9%)	0.01±0.03% (59%)
∞	0.35±0.10% (99.98%)	0.01±0.03% (60%)

Table 3: VFR and ($Pr\{VFR \geq 0\}$) of all countries combined, at $\Delta T = 3$, per data source, with and without prior model.

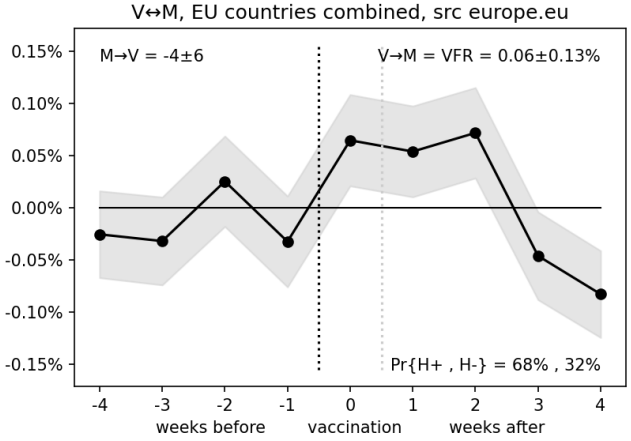

Figure 15: Results for 30 European countries combined, weeks 10-43.

4 Conclusions and discussion

This report presents a causal model of infections, vaccinations and mortality (IVM), with main goal to estimate Vaccine Fatality Ratio VFR on the short-term of a few weeks. The model has few to zero prior model parameters, which are unbiased in terms of causal effect direction (from A to B or vice versa), sign (enforcing or supression, protection or damage), and even strength (strong or weak). Bayesian probabilities are used to quantify all interactions. Five confounders are explicitly taken into account, plus all long-term confounding using a filter that extracts short-term events only. A simpeler VM model without infections and only one “bicausal” interaction is shown to provide essentially the same results, indicating that during the analysis period, infections did not play a significant confounding role.

Evidence was found of a causal effect from vaccination to mortality during booster campaigns in the Netherlands (2022 weeks 9-50) and Europe (weeks 10-43 due to data limtations). A positive Vaccine Fatality Ratio VFR was found within 2-3 weeks after vaccination of 0.13% (0.05%-0.21%, 95% CI) for The Netherlands, and 0.35% (0.05%-0.55%) for Europe. These VFRs transcend the IFR of covid substantially [Io2].

The high VFR on the short-term was found to be partially compensated a few weeks later. A single, partially age-stratified experiment did indicate that vaccine-induced mortality focuses on the 65+ age group. This supports the mechanism of very frail elderly whose death is accelerated 1-2 weeks due to vaccination, associated with a low loss of QALYs (Quality Adjusted Life Years). If present, this mechanism is only partial; VFR over 5 weeks still has 68-80% probability of being net positive.

Additionally, experiments using the IVM model with sewer-viral-particle data in The Netherlands suggested vaccination induces covid-infections and/or reactivates latent viral reservoirs, at a rate scaled to equivalent-PCR-infections per vaccination of 0.50 (0.08-0.92). Recent research reported that infections strongly correlate with vaccinations [Shr].

This study was limited in many ways. The available source data was not case-based but national weekly overall rates. The short-term filter approach is insensitive to all long-term effects. Significance levels were very low for many measurements. The method used is very sensitive for preprocessing that data aggregators may apply, e.g. smoothing or small accidental/deliberate data shifts in time, e.g. to align data sets or optimize visualization. Infection data was of low reliability, by nature. Finally, my method has all kinds of flaws unknown to me, to all [Bre]. Despite all this:

The evidence of a causal relationship from vaccination to infections and mortality is a very strong alarm signal to *stop* the current mass vaccination programs.

References

[Ben] C.S. Benn and F. Schaltz-Buchholzer, “Randomised Clinical Trials of COVID-19 Vaccines: Do Adenovirus-Vector Vaccines Have Beneficial Non-Specific Effects?”, The Lancet preprint, papers.ssrn.com/sol3/papers.cfm?abstract_id=4072489

[Bre] N. Breznau et al., “Observing Many Researchers Using the Same Data and Hypothesis Reveals a Hidden Universe of Uncertainty”, doi.org/10.31222/osf.io/cd5j9

[Eur] Source data for European vaccinations and mortality, europe.eu (ECDC and EuroStat)

[Gia] E.A.L.Gianicolo et al., “Methods for Evaluating Causality in Observational Studies”, ncbi.nlm.nih.gov/pmc/articles/PMC7081045/

[Io1] J.P.A. Ioannidis, “Exposure-wide epidemiology: revisiting Bradford Hill”, doi.org/10.1002/sim.6825

[Io2] J.P.A. Ioannidis, “Infection fatality rate of COVID-19 inferred from seroprevalence data”, dx.doi.org/10.2471/BLT.20.265892

[Mar] I.C. Marschner, “Estimating age-specific COVID-19 fatality risk and time to death by comparing population diagnosis and death patterns: Australian data”, bmcmedresmethodol.biomedcentral.com/articles/10.1186/s12874-021-01314-w

[Med] G. Medema et al., “Presence of SARS-Coronavirus-2 RNA in Sewage and Correlation with Reported COVID-19 Prevalence in the Early Stage of the Epidemic in The Netherlands”, ACS Publications, pubs.acs.org/doi/10.1021/acs.estlett.0c00357

[Mee] R. Meester et al., “COVID-19 vaccinations and mortality - a Bayesian analysis”, dx.doi.org/10.13140/RG.2.2.34443.21285, and “Bayesian analysis of short-term vaccination effects”, dx.doi.org/10.13140/RG.2.2.21276.16001

[Nor] Norwegian review, “Covid-19: Pfizer-BioNTech vaccine is likely responsible for deaths of some elderly patients”, doi.org/10.1136/bmj.n1372

[Owi] Source data for European vaccinations and mortality, ourworldindata.org

[Re1] A. Redert, “Covid-19 vaccinations and all-cause mortality - a long-term differential analysis among municipalities”, dx.doi.org/10.13140/RG.2.2.33994.85447

[Re2] A. Redert, “Short-term Vaccine Fatality Ratio of booster and 4th dose in The Netherlands”, dx.doi.org/10.13140/RG.2.2.29841.30568

[Sch] T. Schetters, “Prof. dr. Theo Schetters: analyse van oversterfte is reden tot zorg over veiligheid mRNA-vaccins”, artsencollectief.nl/prof-dr-theo-schetters-analyse-van-oversterfte-is-reden-tot-zorg-over-veiligheid-mrna-vaccins/

[Shi] M. Shimonovich et al., “Assessing causality in epidemiology: revisiting Bradford Hill to incorporate developments in causal thinking”, doi.org/10.1007/s10654-020-00703-7

[Shr] N.K. Shrestha et al., “Effectiveness of the coronavirus disease 2019 (covid-19) bivalent vaccine”, doi.org/10.1101/2022.12.17.22283625

[Src] Source data for infections (PCR+ and sewer-viral particles), vaccinations and mortality in The Netherlands, cbs.nl (Central Bureau for Statistics) and rivm.nl (Dutch national institute for health and environment)

[Sun] C.L.F. Sun et al, “Increased emergency cardiovascular events among under-40 population in Israel during vaccine rollout and third COVID-19 wave”, www.nature.com/articles/s41598-022-10928-z

[Wik] Wikipedia, “Causality”, en.wikipedia.org/wiki/Causality, accessed Jan 2023